2 ATLAS+CMS DARK MATTER FORUM RECOMMENDA-
3 TIONS

4 Author/contributor list to be added as document is finalized.

5 April 20, 2015

1
Introduction

This is a citation test [HK11].

q

g_q g_{DM} $\chi\,(m_{\mathrm{DM}})$

$Z'\,(M_{\mathrm{med}})$
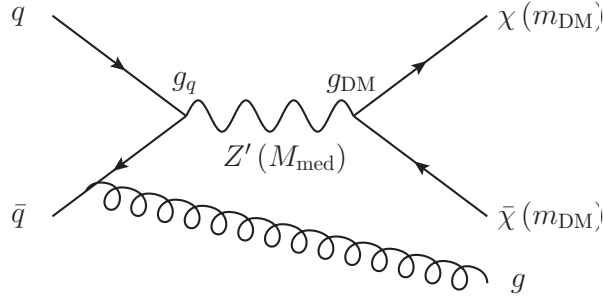
$\bar{q}$ $\bar{\chi}\,(m_{\mathrm{DM}})$

g

Figure 2.1: The diagram shows the pair production of dark matter particles in association with a parton from the initial state via an s-channel vector or axial-vector mediator. The process if specified by $(M_{\mathrm{med}},\,m_{\mathrm{DM}},\,g_{\mathrm{DM}},\,g_q)$, the mediator and dark matter masses, and the mediator couplings to dark matter and quarks respectively.

2

List of simplified models: choices and implementation

General topics:

- choice of Dark Matter type: Dirac (unless specified otherwise) and what we might be missing

- MFV and what we might be missing

2.1 Generic models for mono-jet signatures

Vector and axial vector mediator, s-channel exchange

- Matrix Element implementations (with references)

  - Production mechanism

  - Lagrangian We consider the case of a dark matter particle that is a Dirac fermion and where the production proceeds via the exchange of a spin-1 s-channel mediator. We consider the following interactions between the DM and SM fields including a vector mediator with:
  (a) vector couplings to DM and SM.
  (b) axial-vector couplings to DM and SM.

$$\mathcal{L}_{\text{vector}} = \sum_q g_q Z'_\mu \bar{q} \gamma^\mu q + g_{\text{DM}} Z'_\mu \bar{\chi} \gamma^\mu \chi \tag{2.1}$$

$$\mathcal{L}_{\text{axial}} = \sum_q g_q Z'_\mu \bar{q} \gamma^\mu \gamma^5 q + g_{\text{DM}} Z'_\mu \bar{\chi} \gamma^\mu \gamma^5 \chi \tag{2.2}$$

where the coupling extends over all the quarks and universal couplings are assumed for all the quarks. It is also possible to consider another model in which mixed vector and axial-vector couplings are considered, for instance the couplings to the quarks are vector whereas those to DM are axial-vector. As a starting point, we consider only the models with the vector couplings only and axial vector couplings only. Studies have been performed to see if the case of a mixed coupling can be simply extracted from the other models by some reweighting procedure to take account of the difference in cross section. This would assume that the difference between the pure and mixed couplings case does not affect the kinematics of the event.

– Definition of minimal width We assume that no additional visible or invisible decays contribute to the width of the mediator, this is referred to as the minimal width and it is defined as follows for the vector and axial-vector models.

$$\Gamma_{\text{min}} = \Gamma_{\bar{\chi}\chi} + \sum_q N_c \Gamma_{\bar{q}q} \tag{2.3}$$

where the individual contributions to this from the partial width are from,

$$\Gamma^V_{\bar{\chi}\chi} = \frac{g^2_{\text{DM}} M_{\text{med}}}{12\pi} \left(1 + \frac{2m^2_{\text{DM}}}{M^2_{\text{med}}} \right) \sqrt{1 - \frac{4m^2_{\text{DM}}}{M^2_{\text{med}}}} \tag{2.4}$$

$$\Gamma^V_{\bar{q}q} = \frac{3g^2_q M_{\text{med}}}{12\pi} \left(1 + \frac{2m^2_q}{M^2_{\text{med}}} \right) \sqrt{1 - \frac{4m^2_q}{M^2_{\text{med}}}} \tag{2.5}$$

$$\Gamma^A_{\bar{\chi}\chi} = \frac{g^2_{\text{DM}} M_{\text{med}}}{12\pi} \left(1 - \frac{4m^2_{\text{DM}}}{M^2_{\text{med}}} \right)^{3/2} \tag{2.6}$$

$$\Gamma^A_{\bar{q}q} = \frac{3g^2_q M_{\text{med}}}{12\pi} \left(1 - \frac{4m^2_q}{M^2_{\text{med}}} \right)^{3/2}. \tag{2.7}$$

• Couplings

• Parameter choices (for scan) Vary mediator mass and DM mass

• Generator implementation There are several matrix element implementations of the s-channel vector mediated DM production. This is available in POWHEG, MADGRAPH and also MCFM. The implementation in POWHEG generates DM pair production with 1

parton at Next-to-Leading-Order, whilst Madgraph and MCFM are at leading order. As shown in POWHEG paperHaisch:2013ata, including NLO corrections result in an enhancement in the cross section as compared to leading-order (LO) and though this is not significant, it does lead to a substantial reduction in the dependence on the choice of the renormalisation and factorisation scale and hence the theoretical uncertainty on the signal prediction. Since NLO calculations are available for the process in POWHEG, we recommend to proceed with POWHEG as the generator of choice. In addition to this, studies conducted within the DM forum have shown that POWHEG is more efficient for the generation of events all the way out to the tails of the kinematic distributions (https://indico.cern.ch/event/374678/session/0/material/3/1.pdf). The input configuration in POWHEG allows you to set parameters to not generate events below a given kT cut ('bornktmin') and an additional parameter that ensures sufficient statistics at high transverse momentum ('bornsuppfact). With these flags set to appropriate variables, it is then possible to use a single POWHEG sample to generate the Monte Carlo for all signal regions, whereas with Madgraph more individual samples to be stitched together to achieve the required statistics out to the tails of the kinematic distributions. The POWHEG and Madgraph implementations were compared and the yields obtained from both were found to be compatible.
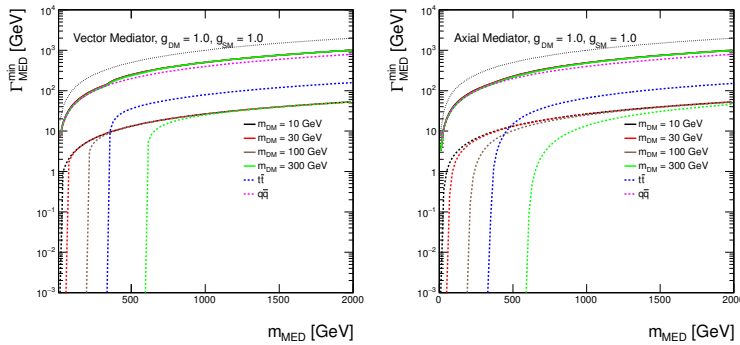

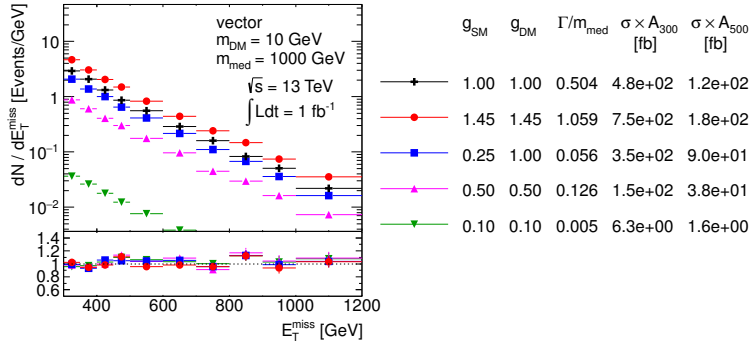Figure 2.2: Scan over couplings
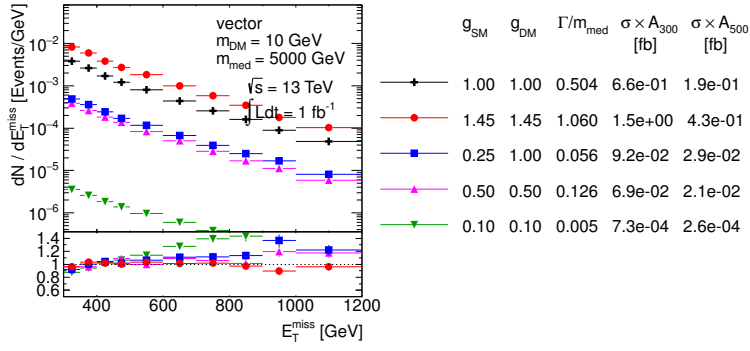
Figure 2.3: Scan over couplings
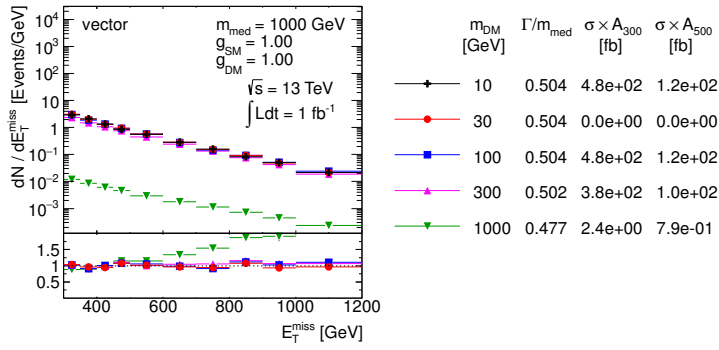

Figure 2.4: Scan over couplings

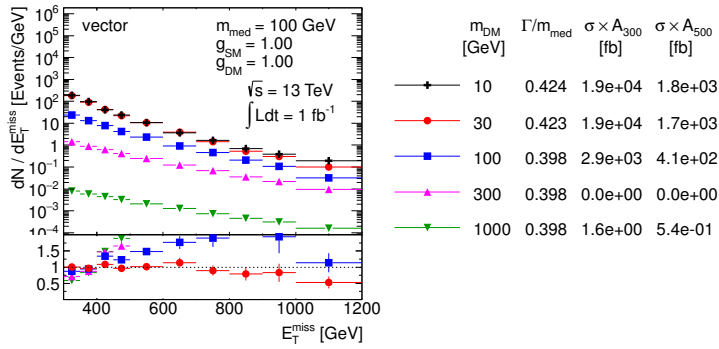Figure 2.5: Scan over Dark Matter mass

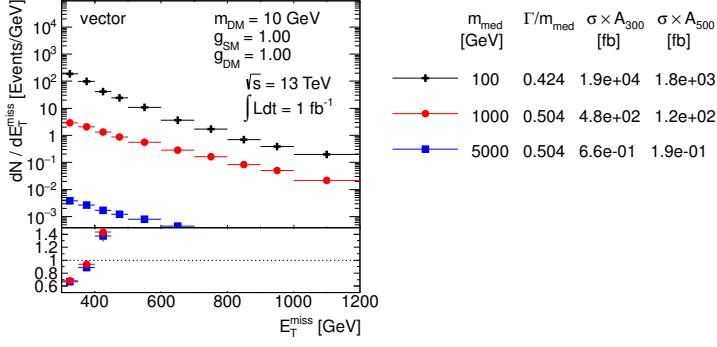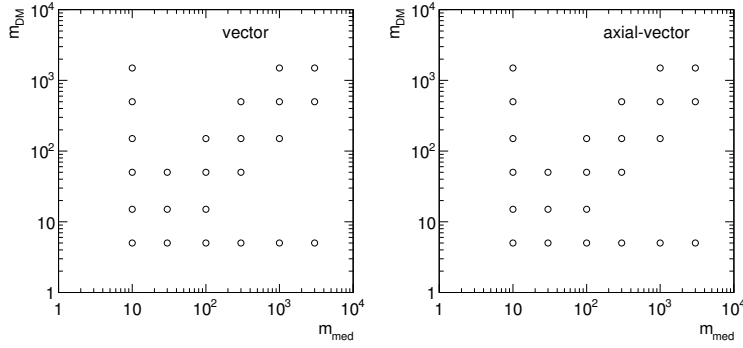Figure 2.6: Scan over Dark Matter mass

Figure 2.7: Scan over mediator mass

Figure 2.8: Parameter grid

Scalar and pseudoscalar mediator, s-channel exchange

$$\Gamma_{\bar{\chi}\chi}^{S} = \frac{g_{DM}^2 M_{med}}{8\pi} \left(1 - \frac{4m_{DM}^2}{M_{med}^2}\right)^{3/2} \tag{2.8}$$

$$\Gamma_{\bar{q}q}^{S} = \frac{3g_q^2 M_{med}}{8\pi} \frac{M_{med} m_q^2}{v^2} \left(1 - \frac{4m_q^2}{M_{med}^2}\right)^{3/2} \tag{2.9}$$

$$\Gamma_{\bar{\chi}\chi}^{P} = \frac{g_{DM}^2 M_{med}}{8\pi} \sqrt{1 - \frac{4m_{DM}^2}{M_{med}^2}} \tag{2.10}$$

$$\Gamma_{\bar{q}q}^{P} = \frac{3g_q^2 M_{med}}{8\pi} \frac{M_{med} m_q^2}{v^2} \sqrt{1 - \frac{4m_q^2}{M_{med}^2}} \ . \tag{2.11}$$

72 *Cross section scaling*

73 *Powheg*

74 • bornktmin and bornsuppfact to ensure sufficient statistics at high

75   MET

76 *MadGraph*

77 • jet differential rates for CKKW for 30 GeV and 80 GeV (ask Fuquan

78   for final plots)
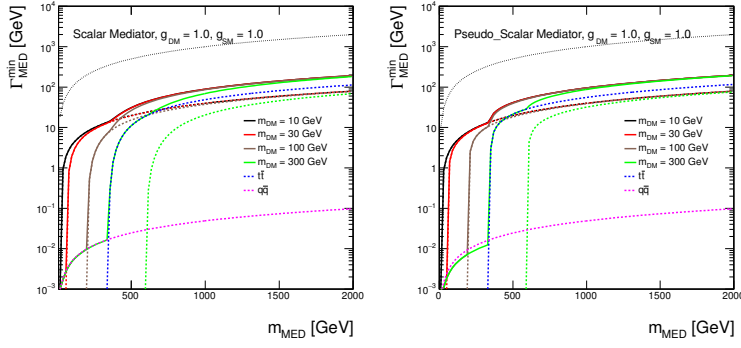
Figure 2.9: Scan over couplings
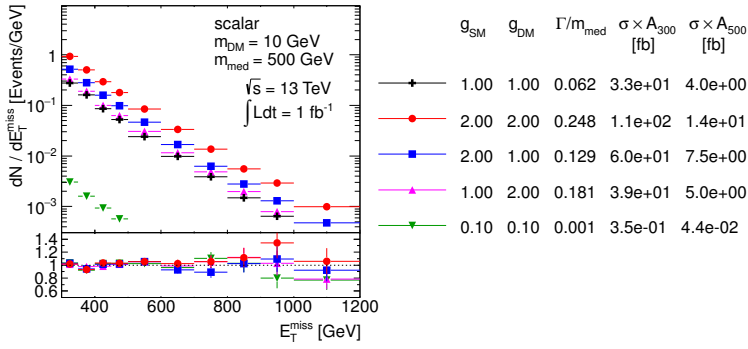
Figure 2.10: Scan over couplings
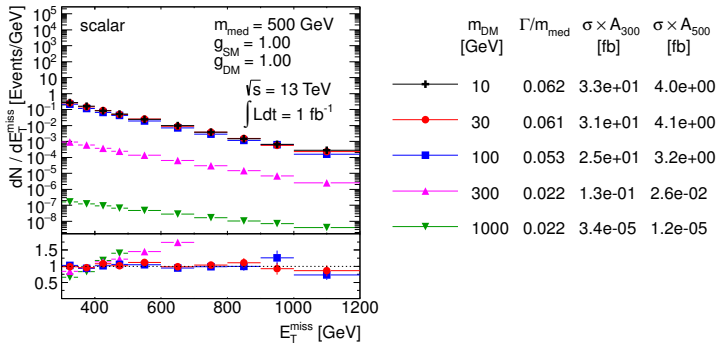
Figure 2.11: Scan over Dark Matter mass
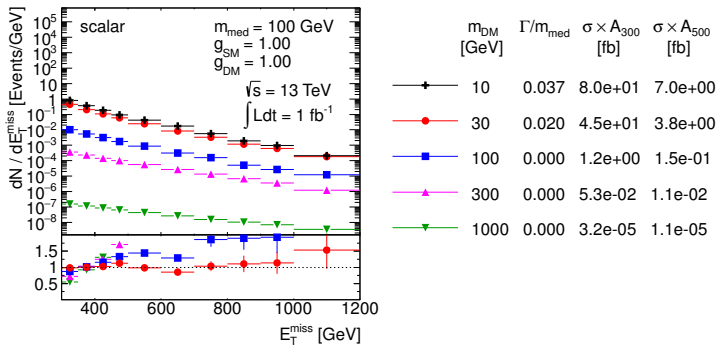
Figure 2.12: Scan over Dark Matter mass
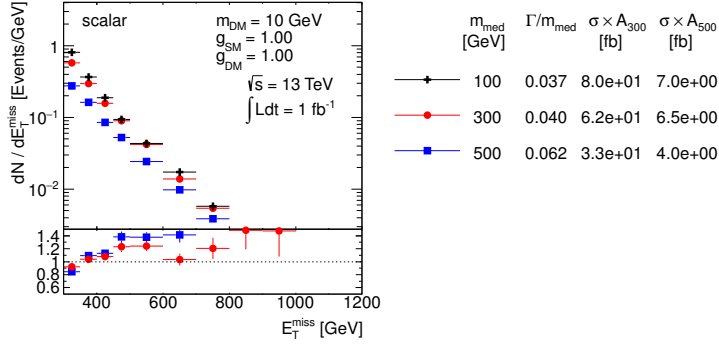
Figure 2.13: Scan over mediator mass
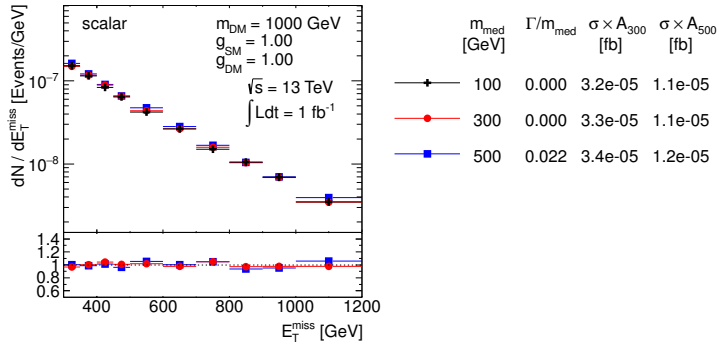
Figure 2.14: Scan over mediator mass
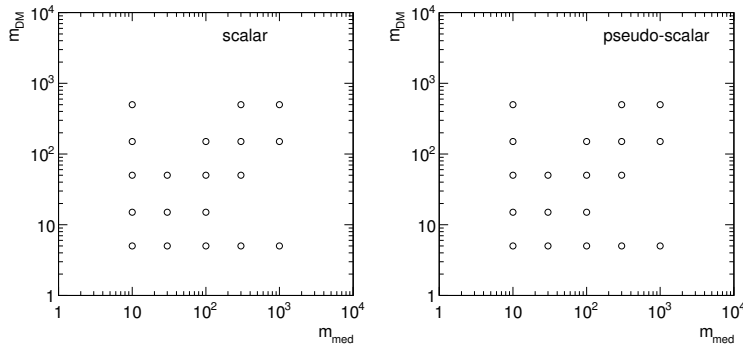
Figure 2.15: Parameter grid
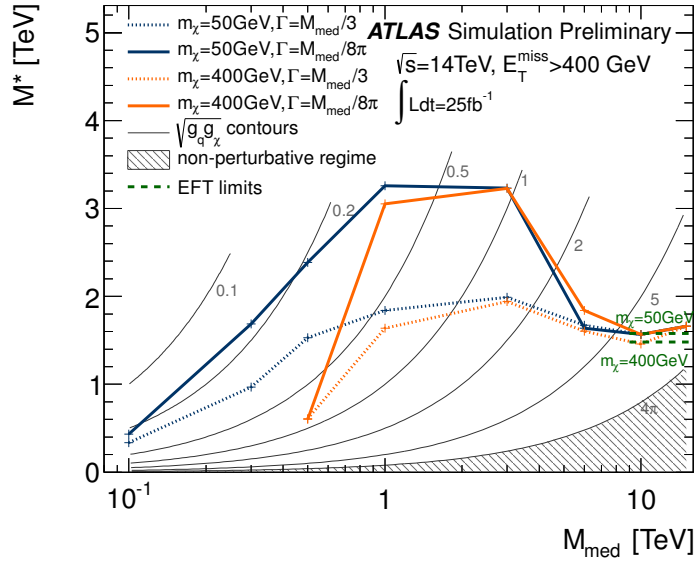
Figure 2.16: Comparison of the 95% CL lower limits on the scale of the interaction of a Z'-like simplified model at 14 TeV, in terms of the mediator mass. Corresponding limits from EFT models are shown on the same plot as green dashed lines to show equivalence between the two models for high mediator masses.
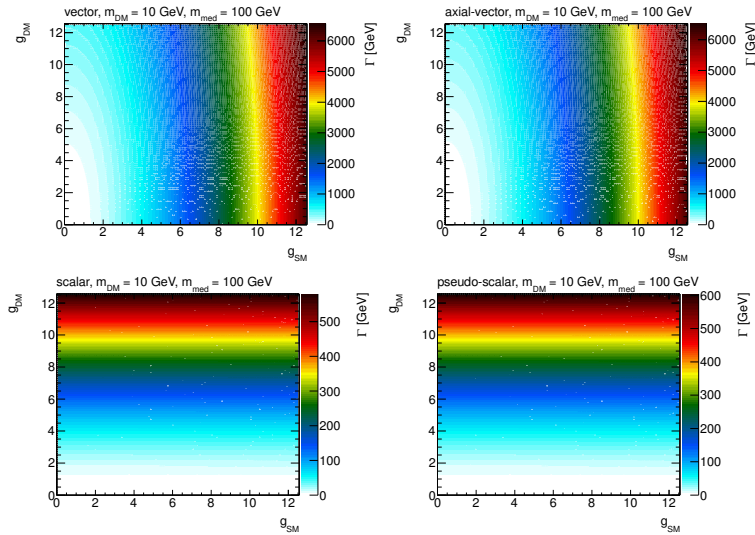
Figure 2.17: Mediator width
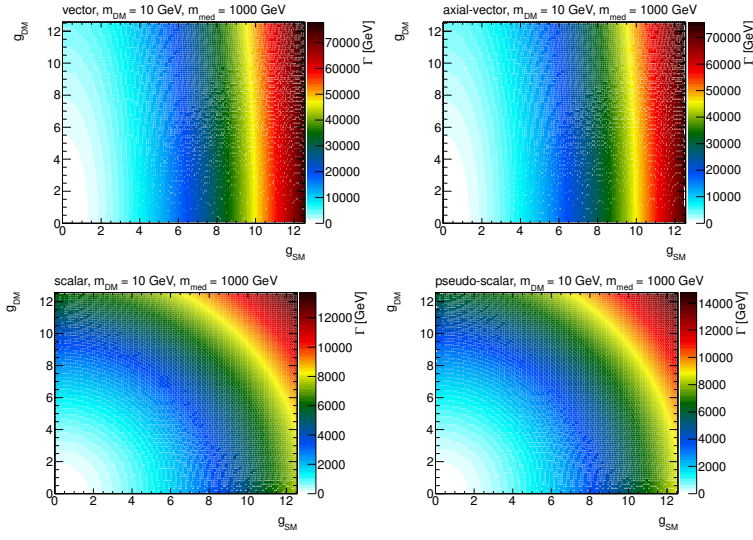
Figure 2.18: Mediator width
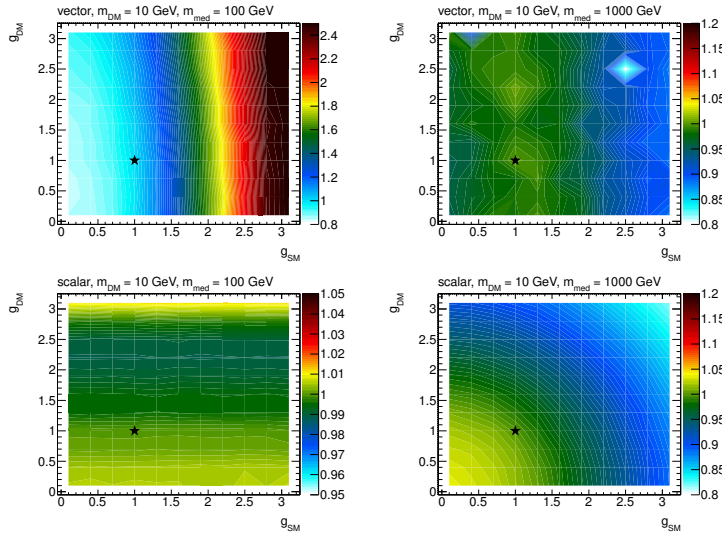
Figure 2.19: Scaling on-shell
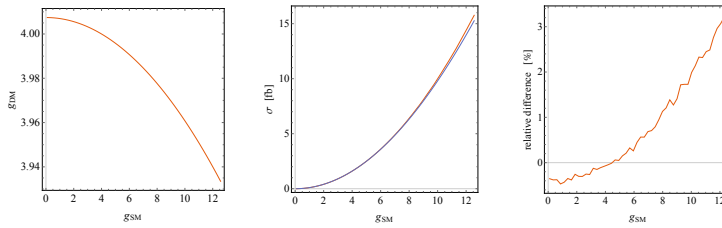
Figure 2.20: Scaling along the lines of constnat width

- 79 • importance of 0-parton sample at low MET with 80 GeV cut

- 80 • 3-parton emission can be ingored (we need new plots with high
- 81   statistics - ask Fuquan or drop this)

82 *Colored scalar mediator, t-channel exchange*   An alternative set of
83 simplified models exist where the mediator is exchanged in the *t*-
84 channel, thereby coupling the quark and dark matter particle directly.
85 Under the assumption that χ is a Standard Model (SM) singlet, the
86 mediating particle, labeled ϕ, is necessarily charged and coloured.
87 This model is parallel to, and partially motivated by, the squark of
88 the MSSM, but in this case the χ is chosen to be Dirac. Following the
89 example of Ref. [PVZ14], the interaction Lagrangian is written as

$$\mathcal{L}_{\text{int}} = g \sum_{i=1,2,3} (\phi_L^i \bar{Q}_L^i + \phi_{uR}^i \bar{u}_R^i + \phi_{dR}^i \bar{d}_R^i)\chi \qquad (2.12)$$

90 (Note: [PVZ14] uses only i = 1,2, but I think it's fine to extend this
91 to 3 here.) where Q_L^i, u_R^i and d_R^i are the SM quarks and ϕ_L^i, ϕ_{uR}^i and
92 ϕ_{dR}^i are the corresponding mediators, which (unlike the *s*-channel
93 mediators) must be heavier than χ. These mediators have SM gauge
94 representations under $(SU(3), SU(2))_Y$ of $(3,2)_{-1/6}$, $(3,1)_{2/3}$ and
95 $(3,1)_{-1/3}$ respectively. Variations of the model previously studied
96 include coupling to the left-handed quarks only [CEHL14, BDSJ$^+$14],
97 to the ϕ_{uR}^i [DNRT13] or ϕ_{dR}^i [PVZ14, A$^+$14b], or some combina-
98 tion [BB13, AWZ14].

99   Minimal Flavour Violation (MFV) requires that the mediator
100 masses for each flavour be equal; the same logic also applies to the
101 couplings g. The available parameters are then

$$\{m_\chi, M_\phi, g\}. \qquad (2.13)$$

102   In practice, the third mediator mass and coupling could be sep-
103 arated from the other two, if higher order corrections to the MFV
104 prediction arise due to the large top Yukawa coupling – a common
105 variation is then to define this split between the first two generations
106 and the third, so the parameters are extended to

$$\{m_\chi, M_{\phi_{1,2}}, M_{\phi_3}, g_{1,2}, g_3\}. \qquad (2.14)$$

107   The width of each mediator is expressed, using the example of

108   decay to an up quark, as

$$\Gamma(\phi_i \to \bar{u}_i \chi) = \frac{g_i^2}{16\pi M_{\phi_i}^3}(M_{\phi_i}^2 - m_{u_i}^2 - m_\chi^2)$$
$$\times \sqrt{M_{\phi_i}^4 + m_{u_i}^4 + m_\chi^4 - 2M_{\phi_i}^2 m_{u_i}^2 - 2M_{\phi_i}^2 m_\chi^2 - 2m_{u_i}^2 m_\chi^2}\,,$$

(2.15)

109   this reduces to

$$\frac{g_i^2 M_{\phi_i}}{16\pi}\left(1 - \frac{m_\chi^2}{M_{\phi_i}^2}\right)^2$$

(2.16)

110   in the limit $M_{\phi_i}, m_\chi \gg m_{u_i}$.

111   An interesting point of difference with the s-channel simplified
112   models is that the mediator can radiate a SM object, such as a jet or
113   gauge boson, thus providing three separate mono-X diagrams which
114   must be considered together in calculations. This model can also
115   give a signal in the di-jet + MET channel when, for example, the χ is
116   exchanged in the t-channel and the resulting ϕ pair each decay to a
117   jet + χ.

118   *2.2   Scalar models*

119   *2.3   Spin-0 Mediators*

120   One of the most straightforward Simplified Models to contemplate
121   is connecting dark matter to the visible sector through a spin-0 me-
122   diator, either a scalar or a pseudoscalar. Such models have intriguing
123   connections with Higgs physics, and can be viewed as generaliza-
124   tions of the Higgs Portal to dark matter. The most general scalar
125   mediator models will of course have renormalizable interactions
126   between the Standard Model Higgs and the new scalar ϕ or pseu-
127   doscalar A, as well as ϕ/A interactions with electroweak gauge
128   bosons. Such interactions are model-dependent, often subject to
129   constraints from electroweak-precision tests, and would suggest spe-
130   cialized searches which cannot be generalized to a broad class of
131   models (unlike the $\not{E}_T$ plus jets searches, for example). As a result,
132   for this class of simplified models with spin-0 mediators, we suggest
133   focusing exclusively on the couplings to fermions, and induced cou-
134   plings to gluons, leaving the possibilities opened up by couplings to
135   the electroweak sector to the discussion of Higgs Portal dark matter.
136   In our benchmark models, we will consider two possibilities for
137   the CP assignment of the mediator (scalar and pseudoscalar), and

two spin-assignments for the dark matter itself (scalar and fermionic). We provide here the Simplified Model for the interactions of the mediator, the relevant equations for scattering with nucleons and self-annihilation, and a discussion of some important issues in simulating events at the LHC. Throughout, we will assume Minimal Flavor Violation (MFV) for the couplings of the mediators to Standard Model fermions.

2.3.1   *Fermionic Dark Matter*

Assuming dark matter is a fermion χ who's interactions with the Standard Model proceed only through a scalar ϕ or pseudoscalar a, the most general Lagrangian at tree-level are

$$\mathcal{L}_{\text{fermion},\phi} \;=\; \mathcal{L}_{\text{SM}} + i\bar{\chi}\slashed{\partial}\chi + m_\chi \bar{\chi}\chi + \left|\partial_\mu \phi\right|^2 + \frac{1}{2}m_\phi^2 \phi^2 + g_\chi \phi \bar{\chi}\chi + \sum_f \frac{g_v y_f}{\sqrt{2}} \phi \bar{f} f \quad (2.17)$$

$$\mathcal{L}_{\text{fermion},a} \;=\; \mathcal{L}_{\text{SM}} + i\bar{\chi}\slashed{\partial}\chi + m_\chi \bar{\chi}\chi + \left|\partial_\mu a\right|^2 + \frac{1}{2}m_a^2 a^2 + i g_\chi a \bar{\chi}\gamma^5 \chi + \sum_f i\frac{g_v y_f}{\sqrt{2}} a \bar{f}\gamma^5 f \quad (2.18)$$

Here, we have made several simplifying assumptions. First, we assume that the coupling to visible-sector fermions is MFV, and proportional to a single universal coupling g_v. Thus, the coupling of ϕ or a to any flavor of fermion f is set by $g_v \times y_f$, where y_f is the Standard Model yukawa $y_f = \sqrt{2}m_f/v$.[1] It is not hard to imagine scenarios that still possess the positive qualities of the MFV assumption but have non-universal g_v; for example, couplings only to up-type quarks, or only to leptons. We do not single out any of these options here in our benchmark models, but remind the reader that it is desirable to have experimental constraints sensitive to couplings to different flavors of fermions. Similarly, since there is no "MFV" motivation for the structure of dark matter-mediator couplings in the dark sector, and it is of course not known whether the dark matter mass m_χ is set by only by the Higgs vev v (indeed this would seem to be somewhat unlikely, given the direct detection constraints on dark matter as containing a pure $SU(2)_L$ doublet) we parametrize the dark matter-mediator coupling by g_χ, rather than by some number times a yukawa coupling proportional to m_χ.

   Finally, the most general Lagrangians including new scalars or pseudoscalars should have a potential V containing possible interactions with the Higgs h. As stated in the introduction, we choose to take a more minimal set of possible interactions, and leave discussions of the Higgs interactions to the sections on the Higgs Portal.

   Given the Lagrangians in Eqs. (2.17) and 2.18, the low-energy Lagrangian will develop loop-level couplings between the mediator ϕ/a and gluons and photons. This proceeds through loops exactly analogous to the loop-level couplings between the Higgs and gluons and

[1] This normalization for the yukawas assumes $v = 246$ GeV and $y_t \sim 1$.

photons. Due to our MFV assumption, as with Higgs physics, the
top quark loop will dominate, with the bottom quark playing a mi-
nor role. Ignoring all couplings except those to the top, the induced
couplings to *on-shell* external gluons and photons are

$$
\mathcal{L}_{\text{loop},\phi} = \frac{\alpha_S}{8\pi}\frac{g_v y_t}{v} f_\phi\left(\frac{4m_t^2}{m_\phi^2}\right)\phi G^{a,\mu\nu}G^a_{\mu\nu} + \frac{\alpha}{8\pi}\left(N_c Q_t^2\right)\frac{g_v y_t}{v} f_\phi\left(\frac{4m_t^2}{m_\phi^2}\right)\phi F^{\mu\nu}F_{\mu\nu}
\tag{2.19}
$$

$$
\mathcal{L}_{\text{loop},a} = \frac{\alpha_S}{4\pi}\frac{g_v y_t}{v} f_a\left(\frac{4m_t^2}{m_\phi^2}\right)a G^{a,\mu\nu}\tilde{G}^a_{\mu\nu} + \frac{\alpha}{4\pi}\left(N_c Q_t^2\right)\frac{g_v y_t}{v} f_a\left(\frac{4m_t^2}{m_\phi^2}\right)a F^{\mu\nu}\tilde{F}_{\mu\nu}
\tag{2.20}
$$

where α_S and α are the QCD and QED fine-structure constants, $N_c =$
3 is the number of quark colors, $Q_t = 2/3$ is the top-quark charge,
and the loop integrals are

$$
f_\phi(\tau) = \begin{cases} \tau\left(1 + (1-\tau)\left[\arcsin\frac{1}{\sqrt{\tau}}\right]^2\right), & \tau < 1, \\ \tau\left(1 + (1-\tau)\left(-\frac{1}{4}\right)\left[\ln\left(\frac{1+\sqrt{1-\tau}}{1-\sqrt{1-\tau}}\right) - i\pi\right]^2\right), & \tau > 1, \end{cases}
\tag{2.21}
$$

$$
f_a(\tau) = \begin{cases} \tau\left[\arcsin\frac{1}{\sqrt{\tau}}\right]^2, & \tau < 1, \\ \tau\left(-\frac{1}{4}\right)\left[\ln\left(\frac{1+\sqrt{1-\tau}}{1-\sqrt{1-\tau}}\right) - i\pi\right]^2, & \tau > 1. \end{cases}
\tag{2.22}
$$

It is important to remember the values of the loop-induced couplings
shown here are correct only in the limit of on-shell external gauge bosons,
and where the internal momenta in the loops are small compared to the
top mass. They should not be used in Monte Carlo even-generation with
gluon jets that have large p_T when compared to m_t, or when the media-
tors themselves have high p_T. The tree-level couplings of scalar and
pseudoscalar mediators to quarks can be used in event-generation
through programs like `MadGraph5` as with any other new physics
model, and model files are available for these purposes. Correct event
generation of scalars/pseudoscalar mediators being produced pri-
marily through the gluon couplings must use more specialized event
generation routines, capable of resolving the loop. Such codes in-
clude `MCFM` and `Sherpa`, but are not as yet ready for out-of-the-box
use in the same manner as `MadGraph`.

These Simplified Models have four free parameters: the universal
coupling g_v, the dark coupling g_χ, the dark matter mass m_χ, and
the mediator mass m_ϕ or m_a. From this, all phenomenology can
be calculated. However, one of the critical derived quantities, the
mediator width, deserves special discussion. Under the minimal

202 model, the widths for the mediators are given by:

$$
\Gamma_\phi = \sum_f N_C \frac{y_f^2 g_v^2 m_\phi}{16\pi}\left(1-\frac{4m_f^2}{m_\phi^2}\right)^{3/2} + \frac{g_\chi^2 m_\phi}{8\pi}\left(1-\frac{4m_\chi^2}{m_\phi^2}\right)^{3/2} \quad (2.23)
$$

$$
+\frac{\alpha_S^2 y_t^2 g_v^2 m_\phi^3}{32\pi^3 v^2}\left|f_\phi\left(\frac{4m_t^2}{m_\phi^2}\right)\right|^2 + \frac{\alpha^2 y_t^2 g_v^2 m_\phi^3}{16\times 9\pi^3 v^2}\left|f_\phi\left(\frac{4m_t^2}{m_\phi^2}\right)\right|^2
$$

$$
\Gamma_a = \sum_f N_C \frac{y_f^2 g_v^2 m_a}{16\pi}\left(1-\frac{4m_f^2}{m_a^2}\right)^{1/2} + \frac{g_\chi^2 m_a}{8\pi}\left(1-\frac{4m_\chi^2}{m_a^2}\right)^{1/2} \quad (2.24)
$$

$$
+\frac{\alpha_S^2 y_t^2 g_v^2 m_a^3}{8\pi^3 v^2}\left|f_a\left(\frac{4m_t^2}{m_\phi^2}\right)\right|^2 + \frac{\alpha^2 y_t^2 g_v^2 m_a^3}{4\times 9\pi^3 v^2}\left|f_a\left(\frac{4m_t^2}{m_a^2}\right)\right|^2
$$

203 Here, the first term in each width corresponds to the decay into Stan-
204 dard Model fermions (the sum runs over all kinematically available
205 fermions, $N_C = 3$ for quarks and $N_C = 1$ for leptons). The second
206 term is the decay into dark matter (assuming that this decay is kine-
207 matically allowed), and the last two terms correspond to decay into
208 gluons and photon pairs. The factor of 2 between the decay into Stan-
209 dard Model fermions and into dark matter is a result of our choice of
210 normalization of the yukawa couplings.

211 In colliders, if the mediator is produced on-shell, as is the primary
212 mode of dark matter production when $m_\chi < m_{\phi/a}/2$ and $m_{\phi/a} \ll \sqrt{\hat{s}}$
213 (where $\sqrt{\hat{s}}$ is some characteristic c.o.m. at the collider in question),
214 the cross section of dark matter production will be proportional to
215 the branching ratio into dark matter. The total production of the me-
216 diator will go as g_v^2, and the decay into invisible dark matter will be
217 $\propto g_\chi^2/\Gamma_{\phi/a}$, with the appropriate kinematic factors. This confounds
218 the easy factorization of limits on the four-dimensional parameter
219 space, since while the total cross section will have an overall depen-
220 dence on the product $g_\chi^2 \times g_v^2$, it will also depend on $\Gamma_{\phi/a}$, which
221 even in the minimal model depends on the sum of g_χ^2 and g_v^2 (with
222 kinematic factors inserted).

223 In addition, as this is a Simplified Model, it is possible that the
224 mediator can decay into additional states present in a full theory
225 that we have neglected. For example, the mediator could decay into
226 additional new charged particles which themselves eventually decay
227 into dark matter, but with additional visible particles that would
228 move the event out of the selection criteria of monojets or similar
229 missing energy searches. Thus, the widths calculated in Eqs. (2.23)
230 and (2.24) are lower bounds on the total width.

231 As a result of these issues, the width of the mediator is often
232 treated as an independent variable in Simplified Models with s-
233 channel production of dark matter. Fortunately, for on-shell produc-
234 tion, the effect of changing the width is only a rescaling of the total
235 event rate assuming that $\Gamma_{\phi/a} < m_{\phi/a}$ [BFG15], which is a necessary

condition for a valid weakly coupled theory. As a result, changing the width just rescales the total event rate at colliders. In the case when the dark matter is produced through an off-shell mediator, the width is not relevant. We therefore recommend that experimental and theoretical bounds on s-channel models make the assumption that the width is minimal, set by Eqs. (2.23) or (2.24), and treat it as a dependent quantity, rather than an additional free parameter.

Furthermore, as we are dealing with a 4D parameter space, it is necessary to consider how to reduce the parameter space to display results which can be compared between experiments and with theory. Clearly, the dependence of the constraints from experiments on the masses m_χ and $m_{\phi/a}$ cannot be suppressed, as the bounds will have non-trivial kinematic dependences on the masses. This leaves the couplings g_χ and g_v. The most straightforward assumption to make is to set $g_\chi = g_v$. This has the somewhat unfortunate result of making certain types of experimental results appear more effective than others. For example, with $g_\chi = g_v$, we expect the mediator branching ratio to dark matter to completely dominate over the visible channels, unless the top channel is kinematically allowed. This would make resonance searches in visible channels for the mediator appear to be uncompetitive. However, some choice must be made, and setting the two couplings equal to each other is perhaps the simplest.

We now turn to the constraints on these models from non-collider experiments: thermal relic abundances, indirect detection, and direct detection. The first two results can be considered together, as they depend on the same set of annihilation cross sections.

Thermal Cross Sections   The thermally-average annihilation of dark matter through the spin-0 mediators can be calculated from the Simplified Model Eqs. (2.17) and (2.18). The resulting cross sections for annihilation into Standard Model fermions, as a function of the dark matter temperature T are

$$\langle \sigma v \rangle (\chi \bar{\chi} \to \phi^* \to f \bar{f}) \;\; = \;\; N_c \frac{3 g_\chi^2 g_v^2 y_f^2 (m_\chi^2 - m_f^2)^{3/2}}{8 \pi m_\chi^2 \left[(m_\phi^2 - 4 m_\chi^2)^2 + m_\phi^2 \Gamma_\phi^2 \right]} T,$$

$$\langle \sigma v \rangle (\chi \bar{\chi} \to a^* \to f \bar{f}) \;\; = \;\; N_c \frac{g_\chi^2 g_v^2 y_f^2}{4 \pi \left[(m_a^2 - 4 m_\chi^2)^2 + m_a^2 \Gamma_a^2 \right]} \left[m_\chi^2 \sqrt{1 - \frac{m_f^2}{m_\chi^2}} + \frac{3 m_f^2}{4 m_\chi \sqrt{1 - \frac{m_f^2}{m_\chi^2}}} T \right].$$

Notably, the scalar mediators do not have a temperature-independent contribution their annihilation cross section, while pseudoscalars do. As $T \propto v^2$, where v is the dark matter velocity, there is no velocity-

independent annihilation through scalars. As, in the Universe today, $v \lesssim 10^{-3}$, this means there are no non-trivial constraints on dark matter annihilation from indirect detection in the scalar mediator model.

The pseudoscalar model, on the other hand, does have relevant constraints from indirect detection. These can be obtained from Eq. 2.25 by setting $T \to 0$, and considering annihilation into the relevant Standard Model channel(s). Most constraints from indirect detection are written in terms of a single annihilation channel, and so the constraints for the full Simplified Model (with multiple annihilation channels open) require some modification of the available results. Good estimates can be obtained by considering the most massive fermion into which the dark matter can annihilate (typically the b or t quark), as this will tend to dominate the annihilation cross section. Note that, outside of resonance, the width is relatively unimportant to the indirect detection constraints.

The thermal relic calculation requires the same input cross sections as the indirect detection. Here, the cross sections are summed over all kinematically available final states, and can be written parametrically as

$$\langle \sigma v \rangle = a + bT.$$

The thermal relic abundance of dark matter is then

$$\Omega_\chi h^2 = \frac{1.04 \times 10^9 \text{ GeV}}{m_{\text{Planck}}} \frac{x_f}{\sqrt{g_\star}} \frac{1}{a + bm_\chi x_f^{-1}}, \tag{2.25}$$

where $x_f \sim 25$ is m_χ over the freeze-out temperature, and g_{star} is the number of degrees of freedom active at the time of freeze-out. For reasonable early Universe parameters, the correct relic abundance occurs when

$$3 \times 10^{-26} \text{ cm}^3/\text{s} = 2.57 \times 10^{-9} \text{ GeV}^{-2} = a + \frac{bm_\chi}{x_f}. \tag{2.26}$$

Keep in mind that these equations require some modification when the dark matter-mediator system is on resonance. Further, recall that we do not know dark matter is a thermal relic, or that the only annihilation process in play in the early Universe is through the mediator. Therefore, while it is appropriate to compare the sensitivity of experimental results to the thermal cross section, this is not the only range of parameters of theoretical interest.

Direct Detection   As noted previously, the scalar mediator model has no indirect detection constraints, while the pseudoscalar does. The situation is reversed in direct detection: the pseudoscalar mediator has no velocity- or momentum-unsuppressed interactions with nucleons, while the scalar mediator induces a spin-independent scattering

cross section. These constraints are very powerful compared to the present collider bounds, especially when $m_\chi > 10$ GeV. As with indirect detection, for weakly coupled theories, the direct detection bounds are relatively independent of the width.

For the scalar mediator model, the interaction with direct detection nuclear targets is (to good approximation) isospin-conserving. Therefore, the bound on scattering with nucleons can be applied to either the dark matter-proton or dark matter-neutron cross section, given by

$$\sigma_{\chi-p,n} = \frac{\mu^2}{\pi} f_{p,n}^2 \tag{2.27}$$

$$f_{p,n} = \sum_{q=u,d,s} f_q^{p,n} \frac{m_{p,n}}{m_q} \left(\frac{g_\chi g_v y_q}{\sqrt{2}m_\phi^2} \right) + \frac{2}{27} f_{\mathrm{TG}}^{p,n} \sum_{q=c,b,t} \frac{m_{p,n}}{m_q} \left(\frac{g_\chi g_v y_q}{\sqrt{2}m_\phi^2} \right) \tag{2.28}$$

where μ is the dark matter-nucleon reduced mass $\mu = (m_\chi m_{p,n})/(m_\chi + m_{p,n})$, and the nuclear matrix elements $f_q^{p,n}$ and $f_{\mathrm{TG}}^{p,n}$ must be extracted from lattice QCD. For our purposes, the neutron and proton matrix elements are essentially identical. Using the values from Ref. [FHZ10] gives (for both protons and neutrons)

$$f_u = 0.02 \tag{2.29}$$
$$f_d = 0.026 \tag{2.30}$$
$$f_s = 0.118 \tag{2.31}$$
$$f_{\mathrm{TG}} = 0.84 \tag{2.32}$$

.

2.4   *Specific models for signatures with EW bosons*

In this Section, we consider models with a photon, a W boson, a Z boson or a Higgs boson in the final state, accompanied by Dark Matter particles that either couple directly to the boson or are mediated by a new particle. The experimental signature is identified as *V+MET*.

These models are interesting both as extensions of models where the gluon provides the experimentally detectable signature, and as stand-alone models with final states that cannot be generated by the models in Section 2.1.

The models considered can be divided in categories:

Models including a contact operator, where the boson is radiated from the initial state
    As depicted in the top diagram of Figure 2.21, these models follow
    the nomenclature and theory for the EFT benchmarks commonly
    used by MET+X searches [GIR$^+$10]. These models have been used
    in past experimental searches [Kha14, Aad14b, K$^+$14, Aad14b,
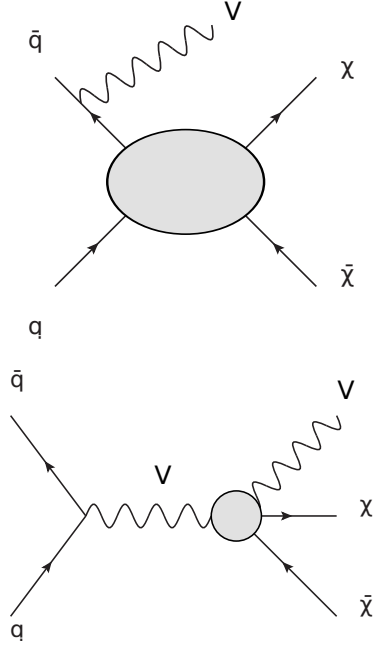   A$^+$14a, Aad14a], and they will not be described here.

Models including a contact operator, where the boson is directly coupled to DM
Shown in the bottom of Figure 2.21, these models allow for a contact interaction vertex that directly couples the boson to Dark Matter.

Simplified models where the boson is radiated from the initial state These models follow those already described in Section 2.1, replacing the initial state gluon with a boson.

V-specific simplified models These models postulate direct couplings of new mediators to bosons, e.g. they couple the Higgs boson to a new scalar [CDM+14].

The following Sections describe the models within these categories, the parameters for each of the benchmark models chosen, the studies towards the choices of the parameters to be scanned, and finally point to the location of their Matrix Element implementation.

SIMPLIFIED MODELS WITH ISR BOSON RADIATION
Searches in the jet+MET final state are generally more sensitive with respect to final states including bosons, due to the much larger rates of signal events featuring quark or gluon radiation with respect to radiation of bosons [ZBW13], in combination with the low branching ratios if leptons from boson decays are required in the final state. The rates for the Higgs boson radiation is too low for these models to be considered a viable benchmark [CDM+14]. However, the presence of photons leptons from W and Z decays and W or Z bosons

decaying hadronically allows to reject the background more effec-
tively, making Z/gamma/W+MET searches still worth comparing
with searches in the jet+MET final state.

Vector mediator exchanged in the s-channel   The case for searches with
W bosons in the final state has so far been strenghtened by the pres-
ence of particular choices of couplings between the WIMP and the up
and down quarks which enhance W radiation [BT13], in the case of
the exchange of a vector mediator in the s-channel. Run-1 searches
have considered three sample cases for the product of up and down
quark couplings to the mediator ξ:

- No couplings between mediator and either up or down quarks ($\xi = 0$);

- Same coupling between mediator and each of the quark types ($\xi = 1$);

- Coupling of opposite sign between mediator and each of the quark types ($\xi = -1$).

The $\xi = -1$ case leads to a large increase in the cross-section of the
process, and modifies the spectrum of missing transverse energy or
transverse mass used for the searches. The sensitivity of the W+MET
search for this benchmark in this case surpasses that of the jet+MET
search. However, as shown in Ref. [BCD$^+$15], the cross-section in-
crease is due to the production of longitudinally polarized W bosons,
as a consequence of a violation of electroweak gauge symmetries.
Unless further particles are introduced (in a fashion similar to the
Higgs boson in the Standard Model), choosing a value of $\xi = -1$
for this simplified model will lead to a manifest violation of unitar-
ity at LHC energies. The simplified model with a vector mediator
exchanged in the s-channel model can still be considered as a bench-
mark for searches with a W boson if $\xi = 1$. We leave the study of
further models with cross-section enhancements due to different
couplings to up and down quarks for studies beyond the early LHC
searches covered in this document. **[TODO: Substitute the following
sentence with Yang Bai's paragraph]**. An example of such model is
the case of both DM and SM Higgs charged under a new U(1)', with
a a small mass mixing between SM Z-boson and the new Zprime.
This leads to different effective DM couplings to u_L and d_L, propor-
tional to their coupling to the Z boson.
    The scan in the parameters that characterize of this model follow
what already detailed in Section 2.1.
    As in the case of the jet+MET models, the width does not have a
significant impact on the kinematic distributions relevant for those

394 searches. An example of the particle-level analysis acceptance us-
395 ing the generator-level cuts from Ref. [Aad15] for the photon+MET
396 analysis, but raising the photon p_T cut to 150 GeV is shown in Fig-
397 ure 2.22, comparing a width that is set to $\Gamma = M_{med}/3$ to the minimal
398 width (the ratio between the two widths ranges from 1.05 to 1.5 with
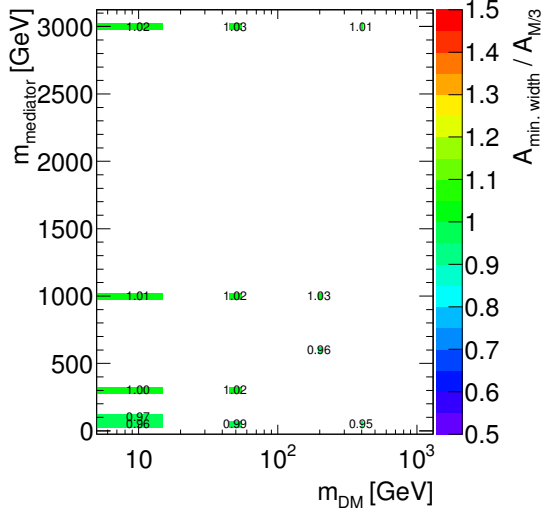399 increasing mediator masses).

Figure 2.22: Analysis acceptance for the photon+MET analysis when varying the mediator width, in the case of a vector mediator exchanged in the $s-$channel

400 Examples of relevant kinematic distributions for selected bench-
401 mark points are shown in Fig. 2.27; leading-order cross-sections for
402 the chosen benchmark points are shown in Table **?? [TODO: Insert**
403 **table of cross-sections]**.

404 *Colored scalar mediator exchanged in the s-channel*   t-channel colored
405 scalar, to be completed...

406 *Model implementation*   These models are generated at leading or-
407 der with MadGraph 2.2.2, and parameter cards can be found on
408 SVN **[TODO: Add SVN location]**. The parton shower is done using
409 Pythia 8, with a matching scale of... **[TODO: To be completed.]**

410 EFT MODELS WITH DIRECT DM-BOSON COUPLINGS
411 A complete list of effective operators with direct DM/boson cou-
412 plings for Dirac DM, up to dimension 7, can be found in [CHLR13].
413 Following the notation of [CNS$^+$13], the dimension 5 benchmark
414 models from this category have a Lagrangian that includes terms
415 such as:

$$\frac{m_W^2}{\Lambda_5^3} \, \bar{\chi}\chi \; W^{+\mu}W_\mu^- + \frac{m_Z^2}{2\Lambda_5^3} \, \bar{\chi}\chi \; Z^\mu Z_\mu \; . \tag{2.33}$$

(a) Missing transverse momentum distribution for the photon+MET final state, for different mediator mass choices, for a DM mass of 10 GeV.

(b) Leading photon transverse momentum distribution for the photon+MET final state, for different DM mass choices, with a mediator mass of 1 TeV.
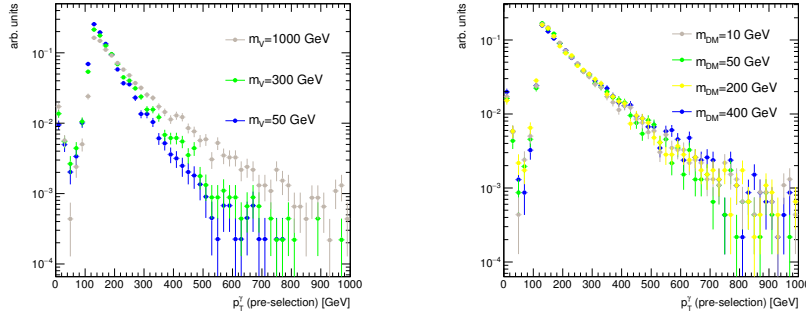
Figure 2.23: Kinematic distributions relevant for searches with W, Z and photons in the final state, for the simplified model with a vector mediator exchanged in the $s-$channel.

(c) Missing transverse momentum distribution for the leptonic Z+MET final state.

(d) Transverse mass (m_T) for the leptonic W+MET final state.

(e) Fat **[Insert algorithm]** jet mass (m_T) for the the hadronic W+MET final state.

where m_Z and m_W are the masses of the Z and W boson, W^μ and Z^μ are the fields of the gauge bosons, χ denote the Dark Matter fields and Λ_5 is the effective field theory scale. This operator induces signatures with MET in conjunction with Z and W bosons at tree level, while at loop level it induces couplings to photon pairs and $Z\gamma$ through W loops. **[TODO: Ask Linda to explain this better than I did.]**. In these models, a clear relation exists between final states with photons, EW bosons and Higgs boson. **[TODO: see if mono-Higgs studies exist for these operators, include them here]**.

The dimension 7 benchmark models include couplings to the

kinetic terms of the EW bosons ($F_i^{\mu\nu}$, with $F_i = 1, 2, 3$ being the field strengths of the SM $U(1)$ and $SU(2)$ gauge groups and $\tilde{F}_i^{\mu\nu}$ their dual tensors). The Lagrangian for the scalar coupling of DM and bosons include terms such as the following:

$$\frac{1}{\Lambda_{7,S}^3} \bar{\chi}\chi \sum_i k_i F_i^{\mu\nu} F_{\mu\nu}^i + \frac{1}{\Lambda_{7,S}^3} \bar{\chi}\chi \sum_i k_i F_i^{\mu\nu} \tilde{F}_{\mu\nu}^i \qquad (2.34)$$

The Lagrangian with pseudoscalar coupling includes the following terms:

$$\frac{1}{\Lambda_{7,PS}^3} \bar{\chi}\gamma^5\chi \sum_i k_i F_i^{\mu\nu} F_{\mu\nu}^i + \frac{1}{\Lambda_{7,PS}^3} \bar{\chi}\gamma^5\chi \sum_i k_i F_i^{\mu\nu} \tilde{F}_{\mu\nu}^i \qquad (2.35)$$

The cut-off scales Λ for the separate terms can be related to operators with different Lorentz structure from Ref. [CHLR13]. Given that they do not lead to substantial differences for collider searches as shown in Figure 2 of Ref. [CNS+13], they have been denoted as $\Lambda_{7,S}$ for the scalar case and $\Lambda_{7,PS}$ for the pseudoscalar case.

The k_i coefficients for the dimension 7 models are related to the couplings of DM to pairs of gauge bosons by gauge invariance:

$$g_{WW} = \frac{2k_2}{s_w^2 \Lambda_7^3} \qquad (2.36)$$

$$g_{ZZ} = \frac{1}{4s_w^2 \Lambda_7^3} \left(\frac{k_1 s_w^2}{c_w^2} + \frac{k_2 c_w^2}{s_w^2} \right) \qquad (2.37)$$

$$g_{\gamma\gamma} = \frac{1}{4c_w^2} \frac{k_1 + k_2}{\Lambda_7^3} \qquad (2.38)$$

$$g_{Z\gamma} = \frac{1}{2s_w c_w \Lambda_7^3} \left(\frac{k_2}{s_w^2} - \frac{k_1}{c_w^2} \right) \qquad (2.39)$$

where s_w and c_w are respectively the sine and cosine of the weak mixing angle.

The coefficients k_i determine the relative importance of each of the boson channels, and their correlations. For example, for what concerns searches with W, Z and photons:

• k_2 alone controls the rate of the coupling to W boson pairs;

• If $k_1 = k_2$ contributions from both Z and γ exchange appear;

• If $k_1 = c_w^2/s_w^2 k_2$ the γ exchange is negligible.

The coefficients k_1 and k_2 are related to the coefficients c_1 and c_2 in the equivalent models of Ref. [CHH15] as $k_2 = s_w^2 * c_2$ and $k_1 = c_w^2 * c_1$.

450   **[TODO: Linda will possibly complete/correct this paragraph]**
451   UV completions of such operators where the dominant signature
452   is a single photon or EW boson are possible, for example through
453   the exchange of a W' or a Z'. They are left as benchmarks for future
454   searches as their implementation may require loop diagrams and
455   need further studies beyond the timescale of this Forum.

456   As shown in Fig. 2.24 kinematics of this model can be approxi-
457   mated by that of a simplified model including a high-mass scalar
458   mediator exchanged in the s-channel. For this reason, the list of
459   benchmark models with direct boson-DM couplings only includes
460   dimension 7 operators. **[TODO: then we need to recommend the**
461   **scalar mediator, but then the sensitivity is very poor wrt monojets**
462   **- however, I still prefer to generate a few (high-mass) simplified**
463   **model points wrt an EFT if given the choice.]**

Figure 2.24: Comparison of the missing transverse momentum for the simplified model where a scalar mediator is exchanged in the s-channel and the model including a dimension-5 scalar contact operator, in the leptonic Z+MET final state

464   The kinematic distributions for dimension-7 scalar and pseu-
465   doscalar operators only shows small differences, as shown in Fig. 2.25.

Figure 2.25: Comparison of the missing transverse momentum for the scalar and pseudoscalar operators with direct interaction between DM and photon, in the photon+MET final state

466   Similarly, the differences in kinematics for the various signatures
467   are negligible when changing the coefficients k_1 and k_2, as shown in
468   Figure **??**. Only the case $k_1 = k_2 = 1$ is generated as benchmark; other
469   cases are left for reinterpretation as they will only need a rescaling of
470   the cross-sections shown in Table **??** **[TODO: add tables with cross**
471   **sections]** for the various Dark Matter mass points considered.

Figure 2.26: Kinematic distributions relevant for searches with W, Z and photons in the final state, for for the scalar and pseudoscalar operators representing direct interactions between DM and bosons.

(a) Missing transverse momentum distribution for the photon+MET final state.

(b) Missing transverse momentum distribution for the leptonic Z+MET final state.

(c) Transverse mass (m_T) for the leptonic W+MET final state.

Examples of relevant kinematic distributions for selected benchmark points are shown in Fig. 2.27.

Specific simplified models   Mono-Higgs, to be completed...

2.5   *Specific models for signatures with heavy flavor quarks*

2.6   *SUSY-inspired simplified models*

(a) Missing transverse momentum distribution for the photon+MET final state.

Figure 2.27: Kinematic distributions relevant for searches with W, Z and photons in the final state, for the simplified model with a vector mediator exchanged in the $s-$channel.

(b) Missing transverse momentum distribution for the leptonic Z+MET final state.

(c) Transverse mass (m_T) for the leptonic W+MET final state.

(d) Fat **[Insert algorithm]** jet mass (m_T) for the the hadronic W+MET final state.

3
Validity of EFT approach

Effective Field Theories (EFTs) are an extremely useful tool for DM searches at the LHC. Given the current lack of indications about the nature of the DM particle and its interactions, a model independent interpretation of the collider bounds appears mandatory, especially in complementarity with the reinterpretation of the exclusion limits within a choice of simplified models, which cannot exhaust the set of possible completions of an effective Lagrangian. However EFTs must be used with caution at LHC energies, where the energy scale of the interaction is at a scale where the EFT approximation can no longer be assumed to be valid. Here we summarise some methods that can be used to ensure the validity of the EFT approximation. These methods are described in detail in Refs. [BDSMR14**?** , BDSJ$^+$14, A$^+$15, RWZ15].

*Outline of the procedure described in Refs. [**?** A$^+$15]*

For a tree-level interaction between DM and the Standard Model (SM) via some mediator with mass M, the EFT approximation corresponds to expanding the propagator in powers of Q_{tr}^2/M^2, truncating at lowest order, and combining the remaining parameters into a single parameter M_* (also called Λ). For an example scenario with a Z'-type mediator (leading to some combination of operators D5 to D8 in the EFT limit) this corresponds to setting

$$\frac{g_{\mathrm{DM}}g_q}{Q_{\mathrm{tr}}^2 - M^2} = -\frac{g_{\mathrm{DM}}g_q}{M^2}\left(1 + \frac{Q_{\mathrm{tr}}^2}{M^2} + \mathcal{O}\left(\frac{Q_{\mathrm{tr}}^4}{M^4}\right)\right) \simeq -\frac{1}{M_*^2}, \qquad (3.1)$$

where Q_{tr} is the momentum carried by the mediator, and g_{DM}, g_q are the DM-mediator and quark-mediator couplings respectively. Similar expressions exist for other operators. Clearly the condition that must be satisfied for this approximation to be valid is that $Q_{\mathrm{tr}}^2 < M^2 = g_{\mathrm{DM}}g_q M_*^2$.

We can use this condition to enforce the validity of the EFT approximation by restricting the signal (after the imposition of the cuts

of the analysis) to events for which $Q_{tr}^2 < M^2$. This truncated signal can then be used to derive the new, truncated limit on M_* as a function of $(m_{DM}, g_{DM}g_q)$.

For the example D5-like operator, $\sigma \propto M_*^{-4}$, and so there is a simple rule for converting a rescaled cross section into a rescaled constraint on M_* if the original limit is based on a simple cut-and-count procedure. Defining σ_{EFT}^{cut} as the cross section truncated such that all events pass the condition $\sqrt{g_{DM}g_q}M_*^{rescaled} > Q_{tr}$, we have

$$M_*^{rescaled} = \left(\frac{\sigma_{EFT}}{\sigma_{EFT}^{cut}} \right)^{1/4} M_*^{original}, \qquad (3.2)$$

which can be solved for $M_*^{rescaled}$ via either iteration or a scan (note that $M_*^{rescaled}$ appears on both the LHS and RHS of the equation). Similar relations exist for a given UV completion of each operator. The details and application of this procedure to ATLAS results can be found in Ref. [A+15] for a range of operators. Since this method uses the physical couplings and energy scale Q_{tr}, it gives the strongest possible constraints in the EFT limit while remaining robust by ensuring the validity of the EFT approximation.

Outline of the procedure described in Ref. [RWZ15]

In [RWZ15] a procedure to extract model independent and consistent bounds within the EFT is described. This procedure can be applied to any effective Lagrangian describing the interactions between the DM and the SM, and provides limits that can be directly reinterpreted in any completion of the EFT.

The range of applicability of the EFT is defined by a mass scale M_{cut}, a parameter which marks the upper limit of the range of energy scales at which the EFT can be used reliably, independently of the particular completion of the model. Regardless of the details of the full theory, the energy scale probing the validity of the EFT is less than or equal to the centre-of-mass energy E_{cm}, the total invariant mass of the hard final states of the reaction. Therefore, the condition ensuring the validity of the EFT is, by definition of M_{cut},

$$E_{\text{cm}} < M_{\text{cut}} . \tag{3.3}$$

For example, in the specific case of a tree level mediation with a single mediator, M_{cut} can be interpreted as the mass of that mediator.

There are then at least three free parameters describing an EFT: the DM mass m_{DM}, the scale M_* of the interaction, and the cutoff scale M_{cut}.

We can use the same technique as above to restrict the signal to the events for which $E_{\text{cm}} < M_{\text{cut}}$, using only these events to derive the exclusion limits on M_* as a function of $(m_{\text{DM}}, M_{\text{cut}})$. We can also define an *effective coupling strength* $M_{\text{cut}} = g_* M_*$, where g_* is a free parameter that substitutes the parameter M_{cut}, and therefore derive exclusions on M_* as a function of (m_{DM}, g_*). This allows us to see how much of the theoretically allowed parameter space has been actually tested and how much is still unexplored; For example, in the Z'-type model considered above, g_* is equal to $\sqrt{g_{\text{DM}} g_q}$. The resulting plots are shown in [RWZ15] for a particular effective operator.

The advantage of this procedure is that the obtained bounds can be directly and easily recast in any completion of the EFT, by computing the parameters M_*, M_{cut} in the full model as functions of the parameters of the complete theory. On the other hand, the resulting limits will be weaker than those obtained using Q_{tr} and a specific UV completion.

4
Recommendations for expressing collider constraints

Bibliography

[A$^+$14a] Georges Aad et al. Search for new particles in events with one lepton and missing transverse momentum in pp collisions at $\sqrt{s}$ = 8 TeV with the ATLAS detector. *JHEP*, 1409:037, 2014.

[A$^+$14b] Jalal Abdallah et al. Simplified Models for Dark Matter and Missing Energy Searches at the LHC. *arXiv:1409.2893*, 2014.

[A$^+$15] Georges Aad et al. Search for new phenomena in final states with an energetic jet and large missing transverse momentum in pp collisions at $\sqrt{s} = 8$ TeV with the ATLAS detector. 2015.

[Aad14a] Search for dark matter in events with a hadronically decaying W or Z boson and missing transverse momentum in pp collisions at $\sqrt{s} = 8$ TeV with the ATLAS detector. *Phys.Rev.Lett.*, 112(4):041802, 2014.

[Aad14b] Search for dark matter in events with a Z boson and missing transverse momentum in pp collisions at $\sqrt{s}$=8 TeV with the ATLAS detector. *Phys.Rev.*, D90(1):012004, 2014.

[Aad15] Search for new phenomena in events with a photon and missing transverse momentum in pp collisions at $\sqrt{s} = 8$ TeV with the ATLAS detector. *Phys.Rev.*, D91(1):012008, 2015.

[AWZ14] Haipeng An, Lian-Tao Wang, and Hao Zhang. Dark matter with t-channel mediator: a simple step beyond contact interaction. *Phys. Rev. D*, 89:115014, 2014.

[BB13] Yang Bai and Joshua Berger. Fermion Portal Dark Matter. *JHEP*, 11:171, 2013.

[BCD$^+$15] Nicole F. Bell, Yi Cai, James B. Dent, Rebecca K. Leane, and Thomas J. Weiler. Dark matter at the LHC: EFTs and gauge invariance. 2015.

[BDSJ$^+$14] Giorgio Busoni, Andrea De Simone, Thomas Jacques, Enrico Morgante, and Antonio Riotto. On the Validity of the Effective Field Theory for Dark Matter Searches at the LHC Part III: Analysis for the *t*-channel. *JCAP*, 1409:022, 2014.

[BDSMR14] Giorgio Busoni, Andrea De Simone, Enrico Morgante, and Antonio Riotto. On the Validity of the Effective Field Theory for Dark Matter Searches at the LHC. *Phys.Lett.*, B728:412–421, 2014.

[BFG15] Matthew R. Buckley, David Feld, and Dorival Goncalves. Scalar Simplified Models for Dark Matter. *Phys.Rev.*, D91(1):015017, 2015.

[BT13] Yang Bai and Tim M.P. Tait. Searches with Mono-Leptons. *Phys.Lett.*, B723:384–387, 2013.

[CDM$^+$14] Linda Carpenter, Anthony DiFranzo, Michael Mulhearn, Chase Shimmin, Sean Tulin, et al. Mono-Higgs-boson: A new collider probe of dark matter. *Phys.Rev.*, D89(7):075017, 2014.

[CEHL14] Spencer Chang, Ralph Edezhath, Jeffrey Hutchinson, and Markus Luty. Effective WIMPs. *Phys. Rev. D*, 89:015011, 2014.

[CHH15] Andreas Crivellin, Ulrich Haisch, and Anthony Hibbs. LHC constraints on gauge boson couplings to dark matter. 2015.

[CHLR13] R.C. Cotta, J.L. Hewett, M.P. Le, and T.G. Rizzo. Bounds on Dark Matter Interactions with Electroweak Gauge Bosons. *Phys.Rev.*, D88:116009, 2013.

[CNS$^+$13] Linda M. Carpenter, Andrew Nelson, Chase Shimmin, Tim M.P. Tait, and Daniel Whiteson. Collider searches for dark matter in events with a Z boson and missing energy. *Phys.Rev.*, D87(7):074005, 2013.

[DNRT13] Anthony DiFranzo, Keiko I. Nagao, Arvind Rajaraman, and Tim M. P. Tait. Simplified Models for Dark Matter Interacting With Quarks. *JHEP*, 1311, 2013.

[FHZ10] A. Liam Fitzpatrick, Dan Hooper, and Kathryn M. Zurek. Implications of CoGeNT and DAMA for Light WIMP Dark Matter. *Phys.Rev.*, D81:115005, 2010.

[GIR+10]   Jessica Goodman, Masahiro Ibe, Arvind Rajaraman, William Shepherd, Tim M.P. Tait, et al. Constraints on Dark Matter from Colliders. *Phys.Rev.*, D82:116010, 2010.

[HK11]   Robert M. Harris and Konstantinos Kousouris. Searches for dijet resonances at hadron colliders. *Int. J. Modern Phys.*, 26(30n31):5005–5055, 2011.

[K+14]   Vardan Khachatryan et al. Search for physics beyond the standard model in final states with a lepton and missing transverse energy in proton-proton collisions at $\sqrt{s} = 8$ TeV. 2014.

[Kha14]   Search for new phenomena in monophoton final states in proton-proton collisions at $\sqrt{s} = 8$ TeV. 2014.

[NCC+14]   Andy Nelson, Linda M. Carpenter, Randel Cotta, Adam Johnstone, and Daniel Whiteson. Confronting the Fermi Line with LHC data: an Effective Theory of Dark Matter Interaction with Photons. *Phys.Rev.*, D89(5):056011, 2014.

[PVZ14]   Michele Papucci, Alessandro Vichi, and Kathryn M. Zurek. Monojet versus the rest of the world I: *t*-channel models. *JHEP*, 2014.

[RWZ15]   Davide Racco, Andrea Wulzer, and Fabio Zwirner. Robust collider limits on heavy-mediator Dark Matter. 2015.

[ZBW13]   Ning Zhou, David Berge, and Daniel Whiteson. Mono-everything: combined limits on dark matter production at colliders from multiple final states. *Phys.Rev.*, D87(9):095013, 2013.